The regulation of cysteine cathepsins and cystatins in human gliomas

ARTICLE *in* INTERNATIONAL JOURNAL OF CANCER · OCTOBER 2012

Impact Factor: 5.09 · DOI: 10.1002/ijc.27453 · Source: PubMed

IJC
International Journal of Cancer

The regulation of cysteine cathepsins and cystatins in human gliomas

Boris Gole[1]*, Peter C. Huszthy[2]*, Mara Popovič[3], Jera Jeruc[3], Youssef S. Ardebili[4], Rolf Bjerkvig[2,5] and Tamara T. Lah[1]

[1] Department of Genetic Toxicology and Cancer Biology, National Institute of Biology, Ljubljana, Slovenia
[2] Department of Biomedicine, University of Bergen, Bergen, Norway
[3] Institute of Pathology, Faculty of Medicine, Ljubljana, Slovenia
[4] Clinical Department of Neurosurgery, University Clinical Centre, Ljubljana, Slovenia
[5] NorLux Neuro-Oncology, Public Research Centre for Health Santé, Luxembourg

Cysteine cathepsins play an important role in shaping the highly infiltrative growth pattern of human gliomas. We have previously demonstrated that the activity of cysteine cathepsins is elevated in invasive glioblastoma (GBM) cells *in vitro*, in part due to attenuation of their endogenous inhibitors, the cystatins. To investigate this relationship *in vivo*, we established U87-MG xenografts in non-obese diabetic (NOD)/severe combined immunodeficiency (SCID)-enhanced green fluorescent protein (eGFP) mice. Here, tumor growth correlated with an elevated enzymatic activity of CatB both in the tumor core and at the periphery, whereas CatS and CatL levels were higher at the xenograft edge compared to the core. Reversely, StefB expression was detected in the tumor core, but it was generally absent in the tumor periphery, suggesting that down-regulation of this inhibitor correlates with *in vivo* invasion. In human GBM samples, all cathepsins were elevated at the tumor periphery compared to brain parenchyma. CatB was also typically associated with angiogenic endothelia and necrotic areas. StefB was mainly detected in the tumor core, whereas CysC and StefA were evenly distributed, reflecting the observations in the xenografts. However, at the mRNA level, no differences in cathepsins and cystatins were observed between the tumor center and the periphery in both human biopsies and xenografts. Interestingly, in human tumors, cathepsin and stefin transcript levels correlated with CD68 and CXCR4 levels, but not with epidermal growth factor receptor (EGFR). Moreover, we reveal for the first time that an elevated StefA mRNA level is a highly significant prognostic factor for patient survival.

Malignant gliomas are the most common tumors of central nervous system in adults. Among them, glioblastoma (GBM) is the most aggressive subtype with a median survival of 12–18 months after initial diagnosis.[1] GBM is characterized by rapid cell proliferation, extensive necrosis, high vascularity and diffuse infiltration into the brain. Invasive cells typically follow white matter fiber tracts and migrate through the *corpus callosum* to invade the contralateral hemisphere. Infiltrative growth prevents complete surgical tumor resection, leading to recurrence and poor prognosis.[1]

The process of glioma cell invasion into the surrounding brain parenchyma is associated with increased focal degradation of extracellular matrix, creating tracts on which cells can migrate.[2,3] Proteolytic enzymes from all major protease families, including cysteine cathepsins, have been shown to play a significant role in the infiltrative growth of these tumors.[3,4] The expression of cysteine cathepsins B, L and S (CatB, CatL and CatS, respectively) increases with glioma malignancy, and they have been implicated in glioma invasion. Furthermore, CatB[5–7] and CatS[8] proved to be independent predictors of patient survival. Several studies emphasized the importance of CatB for tumor invasiveness.[9–11] Although similar findings were reported for CatL[12,13] and CatS,[14] more recent reports argue against their involvement in glioma invasion.[11,15]

The activity of cysteine cathepsins is regulated by several factors, including their endogenous inhibitors of the cystatin family. These are generally comprised by intracellular stefin and extracellular cystatin subfamilies, which both have been

Key words: animal models, cysteine cathepsins, cystatins, glioma, invasion, stefins

Abbreviations: AA: anaplastic astrocytoma; CatB: cathepsin B; CatL: cathepsin L; CatS: cathepsin S; CXCR4: CXC-motif receptor type 4; CysC: cystatin C; eGFP: enhanced green fluorescent protein; EGFR: epidermal growth factor receptor; FBS: foetal bovine serum; GBM: glioblastoma; NOD/SCID: non-obese diabetic/severe combined immunodeficiency; PXA: pleomorphic xanthoastrocytoma; StefA: stefin A; StefB: stefin B

Additional Supporting Information may be found in the online version of this article.

Grant sponsor: Helse-Vest

*B.G. and P.C.H. contributed equally to this work

DOI: 10.1002/ijc.27453
History: Received 18 Nov 2011; Accepted 11 Jan 2012; Online 27 Jan 2012

Correspondence to: Tamara T. Lah, National Institute of Biology, Večna pot 111, SI-1000, Slovenia, Tel.: +386-59-232-703, Fax:+386-1-241-2980, E-mail: tamara.lah@nib.si

implicated in cancer.[16] In brain tumors, cystatin C (CysC) expression decreases with malignant progression toward GBM[17] and a lower expression correlates with shorter disease-free survival of the glioma patients.[18] Previously, we have demonstrated that there are higher levels of stefin B (StefB) protein compared to stefin A (StefA) in GBMs,[6,9] although the latter has not been thoroughly investigated.

In general, decreased levels of cystatins, combined with elevated levels of cysteine cathepsins (an imbalance between proteolytic enzymes and their inhibitors), is suggested to be the mechanism of action of cathepsins in cancer progression.[16,19] This has also been verified in gliomas.[9,17,18] The imbalance is expected at the sites where cathepsins are activated, such as at the invasive edge of the tumors, in apoptotic areas and in areas of neoangiogenesis.[6,20,21] In an *in vitro* GBM spheroid invasion model, the physiological ratio between cathepsins and stefins was shown to be altered.[11] Furthermore, cathepsins are redistributed within the tumor cells, which results in elevated CatB and CatL activity in the invading cells compared to the non-invading GBM cells. However, only the inhibition of CatB impaired the invasion of tumor cells into a collagen matrix. Despite the rapid development of *in vitro* methods, no such model can fully recapitulate the complexity of migration patterns and potential interactions with the tumor microenvironment that are present in the living brain. Therefore, we wanted to confirm our previous findings in an *in vivo* animal xenograft model. In a study describing tumor invasion patterns, Friedl and Wolf (2003)[22] classified GBM migration as mesenchymal chains and/or single cell infiltration. Numerous reports have described the glioma cell infiltration pattern along existing structural elements in the brain parenchyma (such as white matter fiber tracts and the corpus callosum), typically by diffuse, infiltrative single-cell spread.[23] Of note, considerable variations in glioma cell invasion patterns are observed even within the same patient GBM.[20] We have previously shown that when U87-MG spheroids are implanted into rat brains, they grow as well-demarcated tumor nodules connected with narrow bands of cells after the first implantation, whereas in subsequent *in vivo* generations, the growth pattern may change to a more diffuse histological type.[24,25]

In the current study, we aimed to evaluate whether cysteine cathepsins and their endogenous inhibitors not being investigated to a great extent in GBMs so far are differentially expressed at the invading tumor edge compared to the central tumor mass in an orthotopic xenograft model in eGFP-transgenic NOD/SCID mice. Furthermore, we wanted to evaluate and compare the expression patterns of these molecules in human GBMs *in situ*, again focusing on the balance between cysteine cathepsins and stefins; in particular StefA.

Material and Methods

Cell culture and dsRED transduction

The human GBM cell line U87-MG was obtained from ATCC (Manassas VA, USA) and authenticated using DNA short tandem repeat (STR) fingerprinting (data not shown). The U87-MG_{dsRED} sub-line was prepared by transducing the red fluorescent protein dsRED into U87-MG cells by a lentiviral vector pWPXL-dsRED as previously described.[26]

Cells were cultured in dulbecco's modified eagle medium (DMEM) (Sigma-Aldrich, Steinheim, Germany) supplemented with 10% FBS, 1% non-essential amino acids, 1% penicillin/streptomycin, 2.5 mM L-glutamine (all PAA Laboratories, Linz, Austria) at 37°C in humidified atmosphere and 5% CO_2.

Animal model and *in vivo* tumorigenesis

NOD/SCID-eGFP mice (*Mus musculus*) generated by Niclou *et al.* (2008)[26] were used. Those mice accept human glioma xenografts without immunosuppressive treatment and the green fluorescent protein expression in the host tissues facilitates easy separation of mouse and xenotransplanted tissue. The protocol was approved by the local ethical committee (approval no. 2007140) and the procedures were in accordance with the Norwegian Animal Act. During housing, the animals were fed a standard pellet diet and provided water *ad librum*. To generate tumor xenografts, 3×10^5 or 5×10^5 U87-MG or U87-MG_{dsRED} cells were injected intracerebrally 1.5 mm to the right of the sagittal suture and 0.5 mm posterior to the bregma at a depth of 1.5 mm from the dura using a Kopf small animal stereotaxic frame (David Kopf, Tujunga, CA, USA). Thirty-one animals were utilized of which 15 (48%) died during transplantation procedure. No acute post-transplantation mortality was observed (one animal died on day 9 due to causes not related to the experiment). As tumorigenicity *per-se* was not a focus of this study no tumorigenicity controls (*i.e.* mock transplantation with saline) were utilized. To follow tumor development, magnetic resonance imaging (MRI) scans were performed 3, 6 and 8 weeks post-implantation. From the 15 animals remaining, 11 (73%) developed tumors.

The animals were sacrificed with CO_2 inhalation, perfused with 0.9% saline and the whole brain was removed. The brains containing U87-MG implants were used for immunohistochemistry (see protocols below) and brains with U87-MG_{dsRED} implants for preparation of tumor tissue samples for molecular analyses. For that purpose, the dsRED expressing tumor tissue was macroscopically separated from the eGFP expressing host tissue under a UV light-assisted dissection microscope. The tumor tissue was further dissected to separate the tumor center and the tumor periphery. From both regions, separate RNA and protein samples were isolated (see protocols below).

Patients and tumor samples

Patients with high-grade malignant gliomas were operated at the Department of Neurosurgery, University Clinical Centre of Ljubljana, Slovenia. The study was approved by the National Medical Ethics Committee of the Republic of Slovenia (Approval no. 109, 204-6/10/07).

All together, 28 patients were included, 18 (64%) men and 10 (36%) women. Median age was 59.5 years. Tumor

diagnoses were established by standard histopathology protocols at the Institute of Pathology of the Medical Faculty, University of Ljubljana. Twenty-five patients were diagnosed with WHO grade IV gliomas and the other three with grade II–III gliomas. Complete patient diagnosis and tumor sample data are shown in the Supporting Information section (Supporting Information Table S1).

When assessed as feasible by the neurosurgeon, (in seven patients), separate tumor core and tumor periphery tissue samples were taken during operation, intended for RNA- and cathepsin activity analysis. These tissues were evaluated by routine microscopy. Only in two cases we managed to clearly confirm separate tumor periphery and tumor core samples. Therefore, we could not obtain consistent differences or trends between periphery and core tissues on either mRNA- or cathepsin activity levels (data not shown). Otherwise, only one tumor sample was obtained and analyzed.

RNA isolation, reverse transcription, quantitative real-time (DNA)-polymerase chain reaction (PCR)

The tissue samples were homogenized in TRIzol reagent (GIBCO Products, Invitrogen, Grand Island, NY, USA) and RNA was isolated as described by the manufacturer. One microgram of each RNA sample was reverse transcribed to cDNA using High Capacity cDNA Reverse Transcription Kit (Applied Biosystems, Foster City CA, USA) following the manufacturers' protocol.

Quantitative real-time-PCR assays were performed on ABI Prism 7900 HT Sequence Detection System using TaqMan Universal PCR Master Mix. Human glyceraldehyde 3-phosphate dehydrogenase (GAPDH) was used as internal control (all Applied Biosystems). The probes, forward and reverse primers used for detection of gene-specific mRNA of CatB, CatL, StefA, StefB and CysC (Supporting Information Table S2) were designed at National Institute of Biology, Ljubljana and produced by Applied Biosystems. For detection of gene-specific mRNA of CatS, CD68, CXCR4 and EGFR corresponding TaqMan Gene Expression Assays (all Applied Biosystems) were used.

The mRNA data were calculated as $2^{-\Delta\Delta Ct}$ values. Fold differences in mRNA expression levels (F) between tumor center and tumor periphery samples were calculated as in the work by Demuth *et al.* (2008)[27] where $F = 2^{(\Delta Ct\mathrm{TP} - \Delta Ct\mathrm{TC})}$ and $\Delta Ct_{\mathrm{TP}} = Ct_{\mathrm{GAPDH}} - Ct_{\mathrm{target\ gene}}$ in tumor periphery sample and $\Delta Ct_{\mathrm{TC}} = Ct_{\mathrm{GAPDH}} - Ct_{\mathrm{target\ gene}}$ in tumor center sample. $F \geq 1.50$ means higher expression and $F \leq 0.75$ lower expression of the selected gene in the tumor periphery sample. F values between 1.50 and 0.75 are regarded as non-significant differences.

Protein extraction, ELISA tests and activity assays

For protein extraction, tissue samples were homogenized in 50 mM Tris buffer, pH 6.9, supplemented with 0.05% (V/V) Brij 35, 0.5 mM dithiothreitol, 5 mM EDTA, 0.5 mM paramethylsulphonyl fluoride and 10 mM pepstatin A (all Sigma-Aldrich). Total protein concentration was determined using Bio-Rad Protein Assay (Bio-Rad Labs, Munich, Germany) according to manufacturer's protocol.

Human CatB, CatL, CatS, StefA, StefB and CysC sandwich ELISA kits with horseradish peroxidase conjugated detection antibodies were used as suggested by the producer (Prof. Janko Kos, Faculty of Pharmacy, University of Ljubljana). Purified native human CatB, CatL, CatS, StefA, StefB and CysC were used as the standards. The tests detect both precursor and active forms of the cathepsins as well as enzyme–inhibitor complexes.

CatB and CatL activities were measured as described in Gole *et al.* (2009).[11] Specific cathepsin activity was calculated based on the differences in degradation-rate of selective substrate (100 μM Z-RR-AMC for CatB, 100 μM Z-FR-AMC, for CatL; both Bachem, Bubendorf, Switzerland) in the presence or absence of selective inhibitor (60 μM Ca-074, Peptide Institute, Osaka, Japan for CatB, for CatL 2 μM Clik 148, provided by Prof. N. Katunuma, Tokushima Bunri University, Tokyo, Japan). CatS activity was measured as described by Flannery *et al.* (2003)[14] using specific substrate 100 μM Z-VVR-AMC (Peptide Institute, Japan). In all cases the released 7-AMC was measured by spectrofluorimetry at selective wavelenghts[11] (Tecan, Groedig, Austria).

Each activity assay was performed in triplicate, and controls with omitted sample (blanks) were performed. Specific activities were expressed in enzyme units (E.U.) per mg of total protein, with one E.U. being the amount of the enzyme releasing 1 nM of 7-AMC per minute.

Immunohistochemical staining

Whole animal brains with U87-MG implants were fixed in 4% paraformaldehyde, cryoprotected in 30% sucrose, embedded in Tissue-Tek OCT (Sakura Finetek, Zoeterwoude, the Netherlands), frozen and cut in 12-μm sections. For staining, the cryosections were permeabilized for 10 min in ice-cold methanol. Non-specific staining was blocked with 10% FBS with 1% bovine serum albumin for 2 hr. Primary antibodies were as listed: monoclonal mouse anti-human CatB IgG (clone 3E1, 65.1 μg/mL), monoclonal mouse anti-human CatL IgG (clone N135, 153.0 μg/mL), monoclonal mouse anti-human CatS IgG (clone 1E3, 100.0 μg/mL), monoclonal mouse anti-human StefB IgG (clone A6/2, 110.0 μg/mL) and monoclonal mouse anti-human CysC (clone 1A2, 60.7 μg/mL); all provided by Prof. Janko Kos (University of Ljubljana). Sections were incubated with primary antibodies overnight at 4°C. The secondary layer of goat anti-mouse IgG Alexa Fluor 546 (1:200, Molecular Probes, Eugene OR) was applied for 1 hr at room temperature in the dark, then sections were mounted with ProLong Gold Antifade Reagent (Molecular Probes). Negative control staining experiments without primary antibodies (secondary antibody only) and blanks (no antibody) sections were also performed. Native eGFP was expressed in the host tissue and the Alexa Fluor 546-mediated red fluorescence indicated the location of target antigens. Stained sections were observed under a Zeiss LSM 510 confocal microscope, using the ×63-oil immersion objective. To visualize tumor tissue, differentially interfered contrast (microscopy) (DIC) pictures of the same areas were superimposed.

Five micrometers paraffin sections of tumor biopsy samples were prepared according to routine procedures of the Institute of Pathology, University of Ljubljana. The sections were stained in an automated slide staining system (Nexes, Ventana, Tucson AZ, USA). The sections were de-waxed, rehydrated and boiled for 10 min in target retrieval solution (TRS) citrate buffer, pH 6.0 (Dako, Glostrup, Denmark) for antigen retrieval. Primary antibodies used were the same as for staining of cryosections. Non-specific signal was blocked with Ventana Antibody Diluent. Sections were incubated for 30 min at 38°C with primary antibodies. The iWIEV DAB Detection System (Ventana) was used as secondary layer. The slides were counter-stained with Mayer's hematoxylin, fixed and studied under the light microscope.

For staining against StefA, paraffin-embedded U87-MG xenograft- and patient biopsy sections were de-waxed, rehydrated and citrate buffer antigen retrieval was performed in a steam cooker for 25 min. Blocking was done using 5% horse serum in TRIS-buffered saline (TBS) for 1 hr at RT. Primary antibody (mouse anti-human StefA IgG, provided by Prof. Janko Kos) was added at 1:25 dilution, and incubated first for 1 hr at RT, thereafter at 4°C overnight. Secondary antibody was horse-anti-mouse biotinylated IgG (Vector, Burlingame, CA, USA), applied at 1:100 in TBS and detection was performed using the Vector ABC Kit (Vector) using DAB as substrate.

Results

Animal model-tumorigenicity of the U87-MG and U87-MG$_{dsRED}$ lines

U87-MG or U87-MG$_{dsRED}$ cells were inoculated intracerebrally in NOD/SCID-eGFP mice, as described above. Progressive tumor growth was verified by MRI, which revealed well-demarcated, compact lesions, which eventually grew into the contralateral hemisphere (Supporting Information Fig. S1a). The mice remained symptom-free during the incubation period (19–58 days, depending on cell dose; average 44 days). On tumor-caused symptoms, the mice were sacrificed and the brains prepared for analysis. On microscopy, the tumor xenografts were sharply delineated against the host tissue. We observed typical mesenchymal chain type of tumor cell movement into the brain tissue (Supporting Information Figs. S1b and S1c).

Cathepsins and cystatins in xenograft core vs. periphery samples are similar on mRNA, protein and activity levels

Individual RNA and protein samples were prepared from each xenograft core, periphery and normal brain sample from six animals, as described above. ELISA tests and enzyme activity assays showed similar trends (Figs. 1*a* and 1*b*). Only CatB, CatL and StefB were expressed at sufficient levels to be detected by ELISA, with CatB being the most abundant protein in both assays. StefA and CysC levels were below detection limits, whereas low levels of CatS enzyme activity could be seen. Overall, no significant differences were observed between central- and peripheral tumor tissue samples (Figs. 1*a* and 1*b*). Differences in protein levels were seen in most of the individual tumor fractions (*i.e.* central and peripheral area from the same tumor), but with no general trends (data not shown).

Quantitative PCR on reverse transcribed mRNA samples failed to reveal any differences in transcript levels of the enzymes between central and peripheral tumor tissue samples ($0.75 < F < 1.50$), with the exception of StefA. For StefA, expression in the peripheral tumor area was on average 2.86 (± 0.99) fold higher than in the central area. Here however, the intersample variations were very high (Fig. 1*c*). Comparisons of mRNA *vs.* protein and protein *vs.* enzyme activity data revealed no correlations for CatB, CatL or StefB (Fig. 1*d*).

The relative levels of cathepsins to cystatins are elevated at xenograft-host border

Immunohistochemical staining of mouse brain sections harboring U87-MG xenografts (five animals) was performed using mouse anti-human CatB, CatL, CatS, StefA, StefB and CysC antibodies. No cross-reactivity to murine cathepsins and cystatins was found (data not shown). Consistent with ELISA and enzyme activity data, CatB staining was the most intense, followed by lower signal for CatL and CatS (Fig. 2, upper rows). Comparing central and peripheral tumor areas, no clear differences in CatB staining were observed, while CatL and CatS levels were markedly stronger at the periphery than in the tumor center. In contrast, StefB staining (Fig. 2, lower rows, center) was intense in the tumor core, and less so at the periphery. Of note, no StefB was observed at the tumor-host border. StefA was weakly expressed in most of the tumor cells in the xenograft center, although it was more intensely expressed in single scattered cells (Fig. 2, lower rows, left). The tumor border harbored very few (1–2 cells per slide) but strongly stained StefA-positive cells. No difference in CysC expression was observed in the tumor center *vs.* the periphery, which was present only in a few scattered cells (Fig. 2, lower rows left and right).

CatB and CatL are redistributed subcellularly at xenograft periphery

We examined the subcellular localization of cathepsins and their inhibitors in the xenograft center and the periphery. The localization of the most abundant cathepsins, CatB and CatL differed in the central and peripheral areas of the tumor. In the tumor center, both cathepsins were expressed intracellularly in a punctate pattern, presumably corresponding to lysosomes (Fig. 3, upper row). In the tumor periphery; in addition to a similar lysosomal localization, CatB and CatL stained intensely in the extracellular space, most probably representing secreted enzyme deposits (Fig. 3, lower row). We did not observe any differences in the subcellular localization of CatS, which was poorly expressed (data not shown). StefA was weakly expressed in the cytoplasm, but some intense granular spots were also seen, possibly

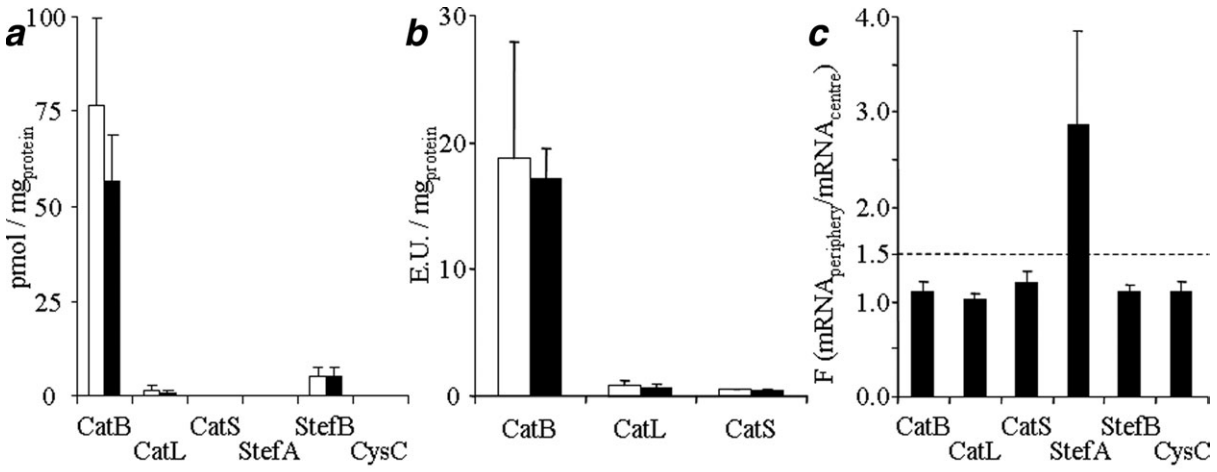

d

value	$CatB_{mRNA}$	$CatB_{activity}$	$CatL_{mRNA}$	$CatL_{activity}$	$StefB_{mRNA}$
r ($CatB_{protein}$)	0,15	0,25			
p	0,708	0,492			
r ($CatL_{protein}$)			-0,21	-0,20	
p			0,917	0,917	
r ($StefB_{protein}$)		0,04		-0,44	-0,52
p		0,964		0,302	0,297

Figure 1. Animal model: cathepsin and cystatin proteins, cathepsin activity and mRNA levels in the central *vs*. peripheral xenograft regions. (*a*) Average protein levels were determined in cell homogenates by ELISA. No significant differences were observed between the central (□) and peripheral (■) regions of the tumors on average ($p > 0.05$, $n = 6$). CatB protein expression was by far the highest. CatS, StefA and CysC were below the detection limit of the ELISA. (*b*) On average, activity levels of the cathepsins did not differ significantly between the central (□) and peripheral (■) regions of the tumors ($p > 0.05$, $n = 6$). CatB activity was by far the highest. (*c*) Fold differences in mRNA expression between central and peripheral tumor regions were calculated as described in Material and Methods section. No differences were observed for CatB, CatL, CatS, StefB and CysC ($0.75 < F < 1.50$, $n = 6$). StefA mRNA levels in tumor periphery were higher than in the tumor center ($F = 2.86 \pm 0.99$). (*d*) Comparing mRNA, protein and activity data revealed no significant correlations between the three levels of expression for CatB, CatL and StefB.

corresponding to lysosomal expression similar to CatB and CatS (see Fig. 2). Cytosolic StefB expression was uniform all over the tumor, except in the cells at the tumor–host border, where no StefB was expressed (see Fig. 2).

Cathepsins and cytatins are up-regulated in human malignant gliomas compared to surrounding brain tissue

In tumor samples from 18 patients out of our cohort of 28 patients, tumor center (tumor tissue without the presence of brain tissue; usually near necroses) and tumor periphery (tumor tissue bordering the infiltrated brain) samples were assessed by hematoxylin/eosin staining (Supporting Information Figs. S1d and 1e). These regions were selected for immunohistochemical analysis of CatB, CatL, CatS, StefA, StefB and CysC. For immunohistochemical scoring, we considered the total number of all immunopositive cells present in the samples and scoring was performed as previously described[6] (presented in Supporting Information Fig. S2 and Table S3).

The immunohistochemical signal of all three cathepsins was significantly lower in the infiltrated normal brain than in the tumor tissue ($p < 0.05$). CatB was present both in the tumor core (Fig. 4*a*) and at the periphery (Fig. 4*b*). Similar to the xenografts, CatB was much more abundant than CatL (Fig. 4*c*) and CatS (Fig. 4*d*). Expression levels of the three inhibitors were also very different. StefA positive cells were found in seven of nine (77.8%) GBM samples analyzed for this marker, of which four samples had low and three had moderate levels. StefA was present in individual cells throughout the tumor, especially close to tumor blood vessels (Fig. 4*e*), and in a population of leukocytes within vessels (data not shown). StefA expressing cells were also found adjacent to small capillaries in the infiltrated brain tissue (Fig. 4*f*). StefB protein was found in only 8 of 18 (44.4%) individual tumor samples, mostly in the central tumor area (Fig. 4*g*), rarely at the periphery; again similar to the xenografts. In contrast to the xenografts, scattered, punctuate StefB expression was seen. On the other hand, CysC was relatively

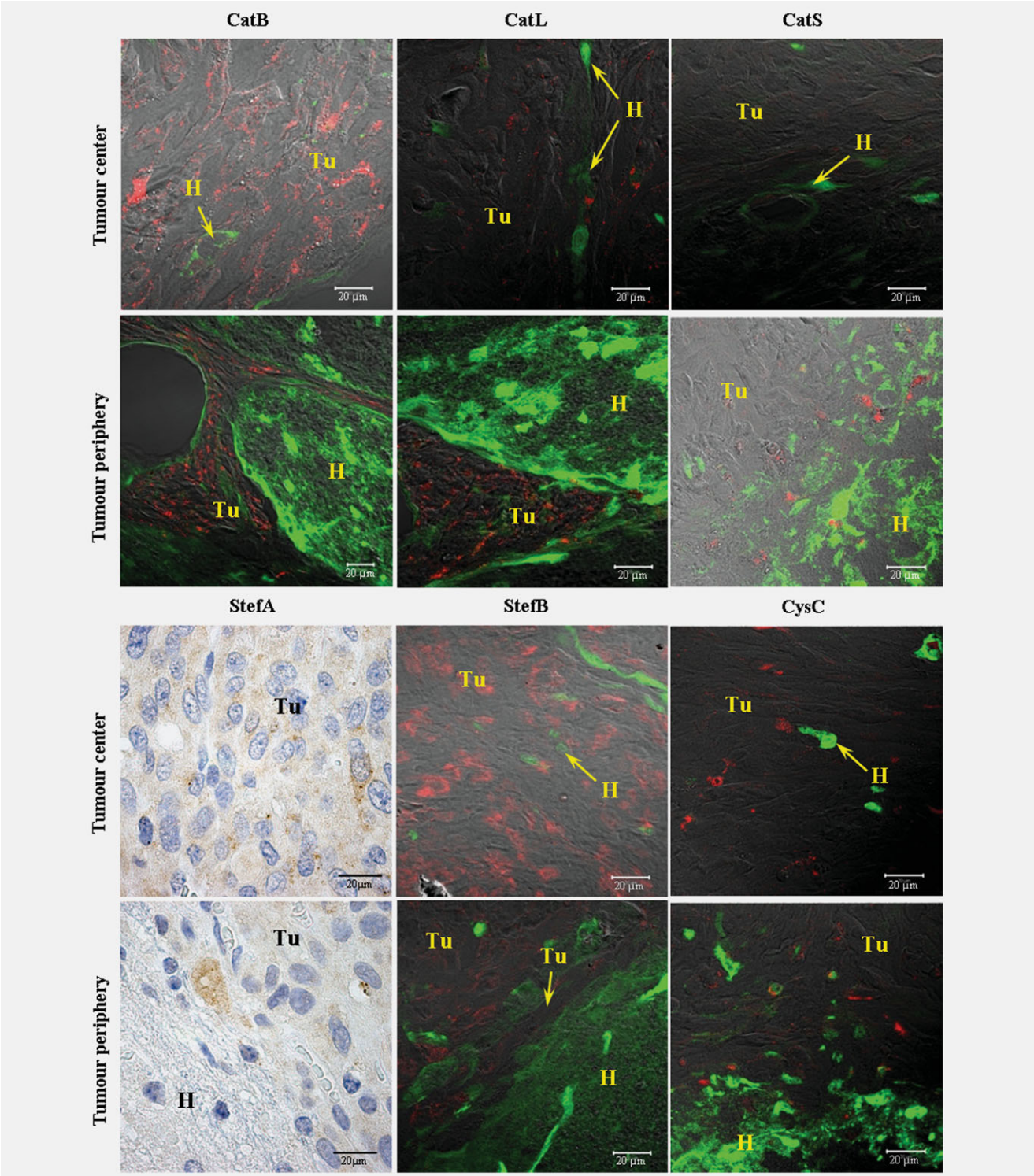

Figure 2. Animal model: immunolabelling of cathepsins and cystatins in U87-MG xenograft regions. Representative samples of the central (above) and peripheral counterparts (below) of the same tumor are shown. Red fluorescence signal indicates localization of CatB, CatL, CatS, StefB and CysC antigens. Host tissue (H) is indicated by green fluorescence and the DIC image of the same areas is superimposed to visualize the tumor (Tu) tissue (confocal microscope, 63× magnified). Different to the above is the image of StefA localization, indicated by brown staining counterstained with hematoxylin (blue staining) to visualize the nuclei (light microscope, 100× magnification). Tumors from five animals were analyzed for each antigen. CatB staining in central and peripheral tumor regions was the most intense compared to the other cathepsins. CatL staining in central tumor regions was weaker than in peripheral regions. Almost no CatS staining was observed in central tumor regions. Also in the periphery regions CatS was the most weakly expressed cathepsin. StefA varied from weak to very strong expression in some of the tumor cells. StefB was strongly expressed in the central tumor regions while less so in the peripheral regions. Practically no StefB was expressed in the cells on the tumor-host border. Only individual cells stained for CysC in the central and the peripheral tumor regions.

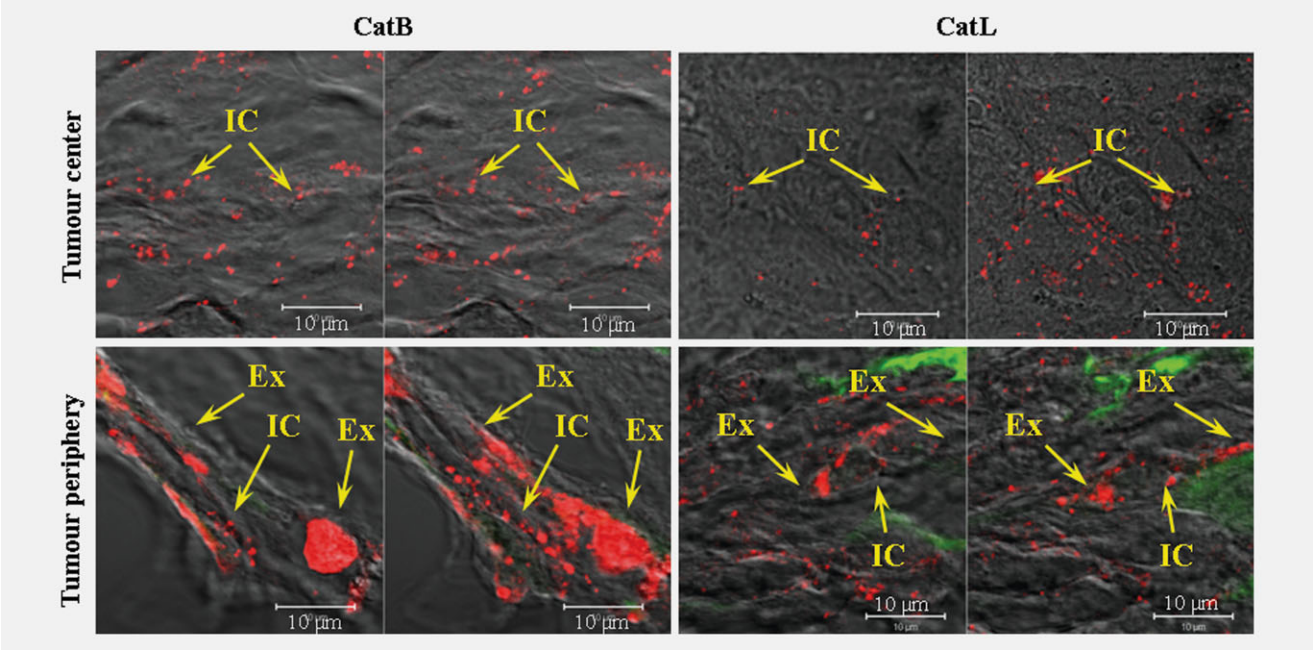

Figure 3. Animal model: intracellular localization of cathepsins B and L. Cryosections of U87-MG tumors in mouse brains stained for human CatB and CatL. Localization of the target antigens is indicated by red fluorescence. Host tissue (H) is indicated by green fluorescence and the DIC image of the same areas is superimposed to visualize the tumor (Tu) tissue (confocal microscope, 63× magnified). Tumors from five animals were analyzed for each antigen. Two successive optical slides of the same areas are presented. In the central tumor regions both CatB and CatL were expressed only in small spots (IC), corresponding to their intracellular (lysosomal) localization. In the peripheral tumor regions, where tumor is growing into the host tissue, CatB and CatL were expressed both intracellularly (IC) and extracellularly (Ex).

well-expressed throughout the tumor tissue (Fig. 4*h*), although in half of the samples, it was preferentially found in central tumor areas. In some tumors, the anti-CysC antibody stained particularly well near the vessels, though not necessarily within endothelial cells (data not shown).

Cathepsin and cystatin mRNA levels correlates with CD68 and CXCR4

Whole RNA extracts were prepared from tumor samples of 24/28 patients with malignant gliomas. The mRNA expression levels of CatB, CatL, CatS, StefA, StefB and CysC were measured. As separate non-invasive tumor center and invasive tumor periphery samples were impossible to obtain for mRNA analysis (see above), and invasive/migratory glioma markers CXCR4 and EGFR,[24] as well as CD68[28] were also measured to obtain an indirect connection to invasiveness. We found that all three cathepsins and both stefins A and B correlated significantly with CD68 and CXCR4 expression (Table 1). CD68 and CXCR4 also correlated with each other, whereas only CatB and CysC levels correlated with EGFR.

StefA and CD68 mRNA levels have prognostic significance in human malignant gliomas

The mRNA expression levels of all three inhibitors and that of CatS also correlated positively to patients' age at the time of operation. Patient age and StefA expression showed a negative correlation with patients' survival time after the first operation (patients' age: $r = -0.43$; $p = 0.042$; for StefA: $r = -0.53$; $p = 0.025$). The survival probabilities confirmed the association between higher patients' age and StefA-expression with shorter survival (Figs. 5*a* and 5*b*), and suggested that CD68 levels are also a prognostic indicator (Fig. 5*c*).

Discussion

The widespread, diffuse single-cell infiltration of malignant glioma cells into the brain makes complete surgical removal of these tumors impossible. This results in tumor recurrence and a low survival rate.[1] As focal degradation of the extracellular matrix by infiltrative "guerrilla cells" is essential to invasion,[22,29,30] extracellular matrix and proteolytic enzyme markers were studied with the aim to find putative anti-invasive targets that would impair disease progression. In previous *in vitro* studies,[27,28] differential transcription profile analyses of invasive *versus* stationary glioma cells revealed a 22-gene signature capable of classifying GBM cell cultures based on their migration rates. These genes were also shown to be affected in 75% of human GBMs.[27] Surprisingly, the markers studied did not include proteolytic enzymes, which have previously been confirmed as key players in GBM progression.[2,4,5,19] Using a

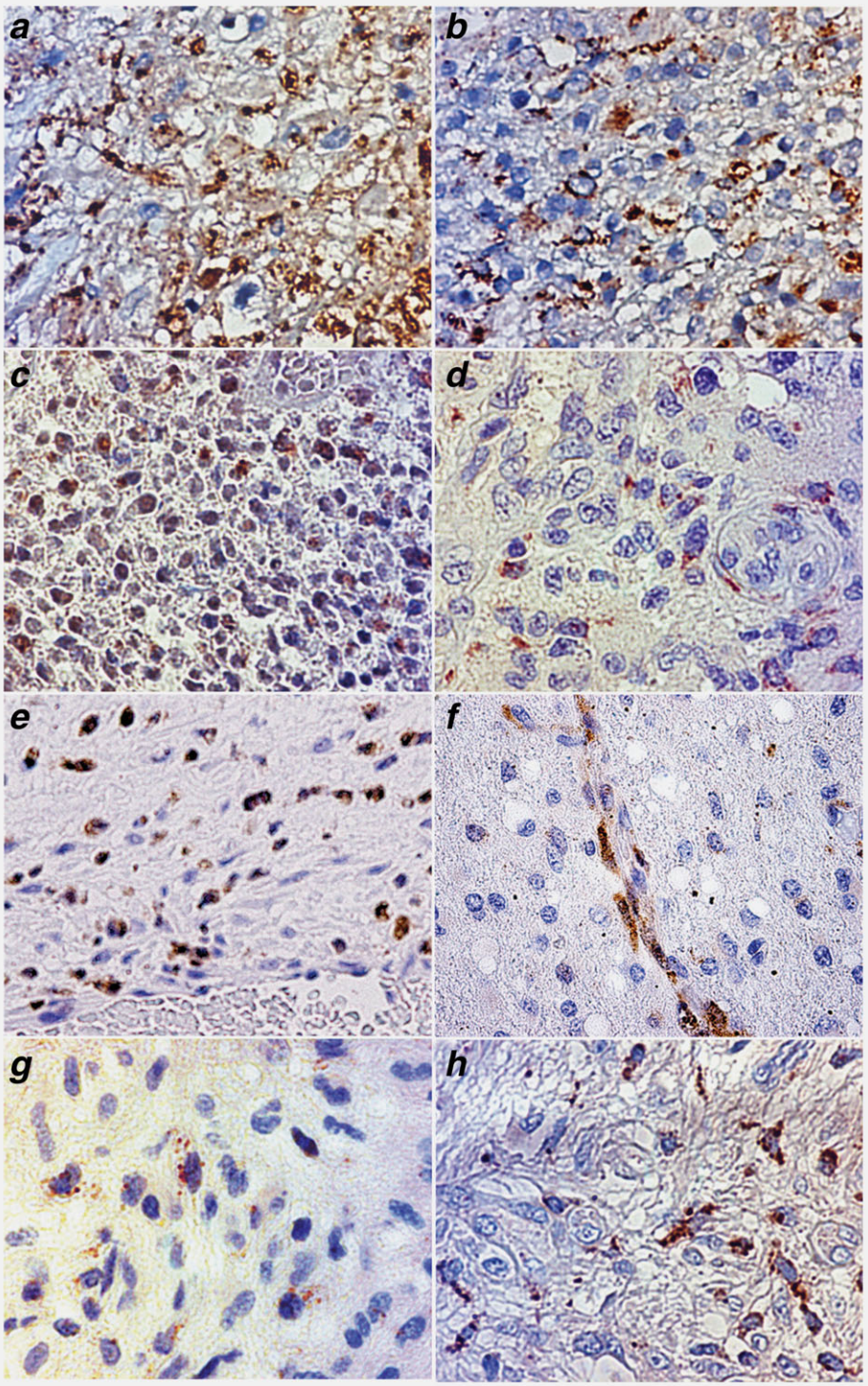

Figure 4. Human glioma: immunohistochemical staining of cathepsins and cystatins. Target proteins are indicated by brown staining counterstained with hematoxylin (blue staining) to visualize the nuclei (light microscope, 100× magnification). Samples from 18 patients were analyzed for each antigen. (*a*,*b*) CatB staining was the strongest among the cathepsins, and present both in tumor periphery (*a*) as well as (*b*) in the tumor center. (*c*) CatL and (*d*) CatS stainings were much weaker. (*e*) StefA stained strongly in individual cells throughout the tumor and (*f*) in particular adjacent to small capillaries. (*g*) StefB staining was faint and present in individual cells mostly in the central regions of the tumors. (*h*) CysC stained throughout the tumor in most of the samples.

Table 1. Correlations at mRNA expression level in human glioma samples

	mRNA								
Value	CatB	CatL	CatS	StefA	StefB	CysC	EGFR	CXCR4	CD68
r (EGFR)	0.47	0.39	0.19	0.00	0.23	0.58		−0.02	0.18
p	0.018	0.053	0.362	0.996	0.301	0.002		0.943	0.401
r (CXCR4)	0.52	0.61	0.50	0.44	0.53	−0.05	−0.02		0.76
p	0.008	0.001	0.013	0.035	0.009	0.815	0.943		<0.001
r (CD68)	0.72	0.76	0.69	0.46	0.79	−0.06	0.18	0.76	
p	<0.001	<0.001	<0.001	0.026	<0.001	0.770	0.401	<0.001	
r (pts age)	0.28	0.36	0.56	0.47	0.53	0.44	−0.03	0.17	0.26
p	0.181	0.086	0.006	0.028	0.011	0.034	0.892	0.434	0.217
r (survival)	−0.02	−0.32	−0.34	−0.53	−0.28	−0.33	−0.26	0.07	−0.08
p	0.945	0.162	0.156	0.025	0.254	0.150	0.268	0.777	0.753

r Spearman's non-arametric correlations of mRNA expression of cathepsins and stefins to mRNA expression of EGFR, CXCR4, CD68, patients' age at initial operation (pts age) and survival time after initial operation.
$p < 0.05$—correlation is statistically significant.

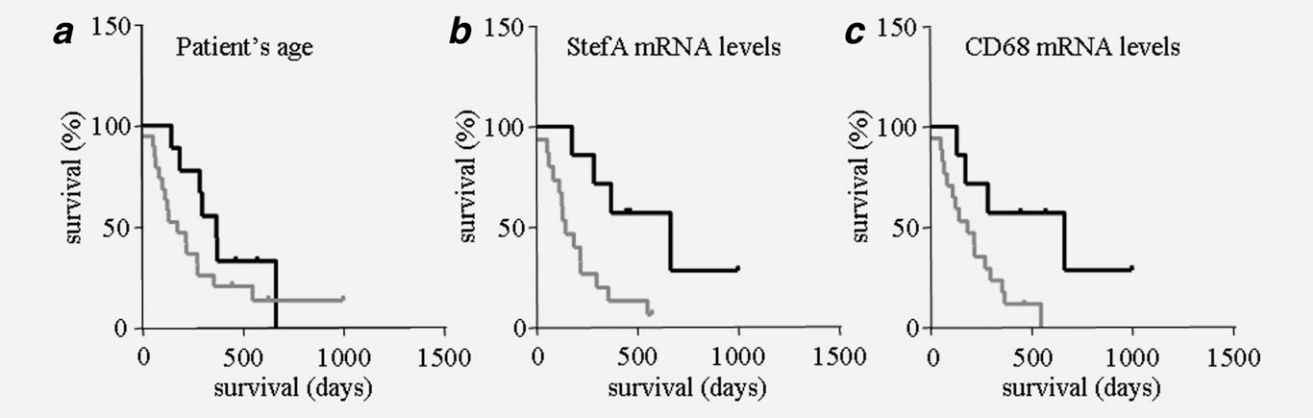

Figure 5. Survival probabilities of patients after initial operations. (*a*) Survival of patients older than 50 years at the time of operation (—) was significantly shorter (median 175 days) than survival of younger patients (—, median 366 days, $p = 0.043$, $n = 24$). (*b*) Survival of patients expressing higher StefA mRNA levels (—, $2^{-\Delta\Delta Ct} > 1.00$) was significantly shorter (median 143 days) than survival of patients with lower StefA mRNA levels (—, median 662 days, $p = 0.014$, $n = 24$). (*c*) Survival of patients expressing higher CD68 mRNA levels (—, $2^{-\Delta\Delta Ct} > 0.50$) was significantly shorter (median 184 days) than survival of patients with lower CD68 mRNA levels (—, median 662 days, $p = 0.046$, $n = 24$).

similar *in vitro* spheroid model as Demuth *et al.* (2008),[27] we recently showed the up-regulation of the activities, but not the mRNA levels of lysosomal cysteine cathepsins B, L and S in invading GBM cells.[11] The up-regulation proved to be the result of post-transcriptional regulation, affecting the protein ratio between these enzymes and their endogenous inhibitors. Of these, mainly intracellular stefin B was attenuated. *In vivo*, cysteine cathepsins may be activated at the tumor cell surface in cells that are in contact with extracellular matrix proteins to induce proteolytic cascade activation facilitating invasion.[31] *In vitro* model is limited, as it describes the infiltration pattern of isolated glioma cells growing in a single extracellular matrix component without contribution of a tumor microenvironment physiology. Thus, the aim of this study was to understand the balance between cathepsins and cystatins *in vivo*, in experimental tumors and in human GBMs.

In our U87-NOD/SCID-eGFP mouse model,[26] the peripheral tumor tissue was well-delineated against the host tissue, similar to what was observed by others in mice[32,33] and rats.[25] U87-MG cells invade by a so called mesenchymal chain type of movement,[23] which is less frequently observed in human GBMs. In separated tumor core *vs.* tumor periphery samples, we failed to find differences in the expression pattern of cysteine cathepsins. This is similar to human GBMs, where we failed to prove differential expression of cathepsins in peripheral *vs.* central tumor parts by immunohistochemistry and at mRNA expression levels. We believe

that this was due mainly to histological heterogeneity of human gliomas.[20,21]

An exception to this is the significantly higher StefA mRNA levels observed in the tumor periphery fraction in xenografts. This however did not translate into higher protein expression, suggesting attenuation of this inhibitor at the translational level. However, total StefA mRNA in human GBM biopsies was a significant ($p = 0.025$) prognostic factor, reported here for the first time. The expression pattern of StefA by immunohistochemistry suggested its presence in leukocytes and inflammatory host cells, in some samples found at high levels in perivascular areas, within vessels and throughout the tumors. Thus, it may suggest that the levels of this inhibitor primarily reflect the level of inflammatory cells, similar to CD68, rather than regulating cathepsin levels in tumor cells. Of note, higher StefA mRNA and protein levels are protective in a mouse model of breast cancer, where it is implicated as an inhibitor of metastasis-promoting cathepsin B.[34] However, due to the excessive amounts of cysteine cathepsins found in normal tissues, the sufficiency of StefA alone to counterbalance protease activity is uncertain.[35] With respect to prognosis, the adverse impact of StefA is similar to what we[36] and others[37] have found in human breast cancer, where we identified StefA as the most significant prognostic factor for disease-free ($p < 0.008$) and overall survival ($p < 0.02$). Later, Parker *et al.* (2008)[34] confirmed that StefA levels, and its ratio to CatB predicted poor survival of breast cancer patients, similar to what Sinha *et al.* (2002)[38] reported in prostate carcinoma. However, an extended population of GBM patients should be analyzed to confirm the prognostic relevance of the StefA transcript.

For comparative cell labeling, we used selected tumor marker genes, such as EGFR,[24] the invasive glioma cell marker CXCR4[39] and CD68, a macrophage/microglial cell marker, which we previously found abundantly present in GBMs.[40] Interestingly, we found a good correlation between the transcripts of all three cathepsins and both stefins with CD68 and CXCR4, but not with EGFR. CD68 and CXCR also correlated to each other. CD68 and CXCR4 are migratory cell markers in gliomas[28] and therefore our finding indirectly supports the notion of involvement of cysteine cathepsin-mediated proteolysis in cell migration and invasion. Although we only analyzed a limited cohort of 24 GBM patients, we managed to validate the previously reported[40] highly significant correlation of CD68 expression with poor survival. However, CatB mRNA did not correlate with prognosis, contrasting reports by Colin *et al.*[41] Taken together, our data suggest that post-translational activation, occurring selectively in the invasive cells, may have strongest impact on regulation of CatB activity during GBM progression, as we have shown *in vitro*.[11]

Additionally, increased focal activity of cathepsins may also be due to their observed translocation to the plasma membrane and secretion of cathepsins from the invasive cells.[5,19–21,42] In the animal model, we observed that CatL and CatS were more frequently localized to the tumor periphery than to the tumor center; in addition to the previously reported CatB.[6,19,21,35,42] Similarly, all three cathepsins were reported at the invasive front in a mouse model of pancreatic islet cell carcinogenesis.[43] CatB was abundantly present throughout the xenograft tissue, similar to human GBMs. Here, we found intense intra-tumoral CatB staining in central necrotic areas as well as in endothelial cells of tumor capillaries,[6,41] indicating its involvement in the angiogenic process. Reversely, in the xenografts and in human GBMs, cytosolic staining of the most abundant inhibitor, StefB, was weaker at the tumor periphery and nearly devoid at tumor border, supporting the notion of an imbalance in the distribution of cathepsin antagonists within the tumor.[5,16,19]

The application of experimental tumor xenografts also allowed us to investigate the subcellular localization of the cathepsins and cystatins. We observed that both CatB and CatL were partially translocated to the surface of the cells at the tumor periphery, consistent with our *in vitro* model study.[11] Moreover, we found spread patches of deposited cathepsins in the extracellular space at the xenograft periphery. In contrast, in the central areas of xenografts punctuate lysosomal cathepsin distribution was observed. These data support previous findings on partial translocation of CatB to the cell surface in gliomas[21] and its association with invasiveness, observed in breast cancer cells[31,35] and in melanoma as well.[44]

In conclusion, we report here on an altered balance between cysteine cathepsins and cystatins at the periphery *vs.* central parts of human GBMs and U87-MG xenografts. The imbalance is in part due to differential translocation and secretion of cathepsins at the tumor border. Our data suggest that post-translational events lead to higher cathepsin activity in the peripheral regions of human GBMs. This finding needs to be reconfirmed, possibly through the use of activity-based probes and laser micro-dissection technology. A further novel finding is the peripheral localization of the inhibitor StefA transcript in U87-MG xenografts and its association with poor GBM prognosis.

Acknowledgements

Authors are grateful to Prof. Dr. Vincenc V. Dolenc (Clinical department of Neurosurgery, University Clinical Centre, Ljubljana, Slovenia) for his contribution to this study's design and organization of patients' samples, Prof. Dr. Janko Kos (Faculty of Pharmacy, University of Ljubljana, Slovenia) for providing the ELISA kits and primary antibodies, Prof. Dr. Nobuhiko Katunuma (Tokushima Bunri University, Tokyo, Japan) for providing Clik 148, Monika Primon (National Institute of Biology, Ljubljana, Slovenia) for U87-MG authentication, Agnete Svendsen (Department of Biomedicine, University of Bergen, Norway) for help with U87-MG_{dsRED} transduction and purification, Dr. Frits Thorsen (Department of Biomedicine, University of Bergen, Norway) for useful suggestions about the MRI scans. Dane Velkovrh (Institute of Pathology, Faculty of Medicine, University of Ljubljana, Slovenia) and Ingrid S. Gavlen (Department of Biomedicine, University of Bergen) are acknowledged for assistance with immunohistochemical staining. The animal breeding facility at the Department of Pathology and the Vivarium (both, University of Bergen) is acknowledged for animal breeding and care. P.C.H was supported by Helse-Vest.

References

1. Louis DN, Ohgaki H, Wiestler OD, Cavenee WK, Burger PC, Jouvet A, Scheithauer BW, Kleihues P. The 2007 WHO classification of tumours of the central nervous system. *Acta Neuropathol* 2007;114:97–109.
2. Rao JS. Molecular mechanisms of glioma invasiveness: the role of proteases. *Nat Rev Cancer* 2003;3:489–501.
3. Demuth T, Berens M. Molecular mechanisms of glioma cell migration and invasion. *J Neurooncol* 2004;70:217–28.
4. Levičar N, Nuttall RK, Lah TT. Proteases in brain tumour progression. *Acta Neurochir (Wien)* 2003; 145:825–38.
5. Lah TT, Durán Alonso MB, Van Noorden CJ. Antiprotease therapy in cancer: hot or not? *Expert Opin Biol Ther* 2006;6: 257–79.
6. Strojnik T, Kos J, Zidanik B, Golouh R, Lah T. Cathepsin B immunohistochemical staining in tumor and endothelial cells is a new prognostic factor for survival in patients with brain tumors. *Clin Cancer Res* 1999;5:559–67.
7. Strojnik T, Kavalar R, Trinkaus M, Lah TT. Cathepsin L in glioma progression: comparison with cathepsin B. *Cancer Detect Prev* 2005;29: 448–55.
8. Flannery T, McQuaid S, McGoohan C, McConnell RS, McGregor G, Mirakhur M, Hamilton P, Diamond J, Cran G, Walker B, Scott C, Martin L, et al. Cathepsin S expression: an independent prognostic factor in glioblastoma tumours—a pilot study. *Int J Cancer* 2006;119: 854–60.
9. Lah TT, Strojnik T, Levicar N, Bervar A, Zajc I, Pilkington G, Kos J. Clinical and experimental studies of cysteine cathepsins and their inhibitors in human brain tumors. *Int J Biol Markers* 2000; 15:90–3.
10. Lakka SS, Gondi CS, Yanamandra N, Olivero WC, Dinh DH, Gujrati M, Rao JS. Inhibition of cathepsin B and MMP-9 gene expression in glioblastoma cell line *via* RNA interference reduces tumor cell invasion, tumor growth and angiogenesis. *Oncogene* 2004;23:4681–9.
11. Gole B, Durán Alonso MB, Dolenc V, Lah T. Post-translational regulation of cathepsin B, but not of other cysteine cathepsins, contributes to increased glioblastoma cell invasiveness *in vitro*. *Pathol Oncol Res* 2009;15:711–23.
12. Sivaparvathi M, Yamamoto M, Nicolson GL, Gokaslan ZL, Fuller GN, Liotta LA, Sawaya R, Rao JS. Expression and immunohistochemical localization of cathepsin L during the progression of human gliomas. *Clin Exp Metastasis* 1996;14: 27–34.
13. Levičar N, Dewey RA, Daley E, Bates TE, Davies D, Kos J, Pilkington GJ, Lah TT. Selective suppression of cathepsin L by antisense cDNA impairs human brain tumor cell invasion *in vitro* and promotes apoptosis. *Cancer Gene Ther* 2003; 10:141–51.
14. Flannery T, Gibson D, Mirakhur M, McQuaid S, Greenan C, Trimble A, Walker B, McCormick D, Johnston PG. The clinical significance of cathepsin S expression in human astrocytomas. *Am J Pathol* 2003;163:175–82.
15. Zajc I, Hreljac I, Lah T. Cathepsin L affects apoptosis of glioblastoma cells: a potential implication in the design of cancer therapeutics. *Anticancer Res* 2006;26:3357–64.
16. Kos J, Lah TT. Cystatins in cancer. In: Zerovnik E, Kopitar-Jerala N, eds. Human stefins and cystatins. New York: Nova Science Publishers Inc., 2006. 153–65.
17. Konduri SD, Yanamandra N, Siddique K, Joseph A, Dinh DH, Olivero WC, Gujrati M, Kouraklis G, Swaroop A, Kyritsis AP, Rao JS. Modulation of cystatin C expression impairs the invasive and tumorigenic potential of human glioblastoma cells. *Oncogene* 2002;21:8705–12.
18. Nakabayashi H, Hara M, Shimuzu K. Clinicopathologic significance of cystatin C expression in gliomas. *Hum Pathol* 2005;36: 1008–15.
19. Lah TT, Obermajer N, Durán Alonso MB, Kos J. Cysteine cathepsins and cystatins as cancer biomarkers. In: Edwards D, Hoyer-Hansen G, Blasi D, Sloane BF, eds. The cancer degradome. Proteases and cancer biology. New York: Springer Science, 2008. 585–623.
20. Rempel SA, Rosenblum ML, Mikkelsen T, Yan PS, Ellis KD, Golembieski WA, Sameni M, Rozhin J, Ziegler G, Sloane BF. Cathepsin B expression and localization in glioma progression and invasion. *Cancer Res* 1994;54:6027–31.
21. Demchik LL, Sameni M, Nelson K, Mikkelsen T, Sloane BF. Cathepsin B and glioma invasion. *Int J Dev Neurosci* 1999;17:483–94.
22. Friedl P, Wolf K. Tumour-cell invasion and migration: diversity and escape mechanisms. *Nat Rev Cancer* 2003;3:362–74.
23. Claes A, Idema AJ, Wesseling P. Diffuse glioma growth: a guerilla war. *Acta Neuropathol* 2007; 114:443–58.
24. Chin L, Gray JW. Translating insights from the cancer genome into clinical practice. *Nature* 2008;452:553–63.
25. Strojnik T, Kavalar R, Lah TT. Experimental model and immunohistochemical analyses of U87 human glioblastoma cell xenografts in immunosuppressed rat brains. *Anticancer Res* 2006;26:2887–900.
26. Niclou SP, Danzeisen C, Eikesdal HP, Wiig H, Brons NH, Poli AM, Svendsen A, Torsvik A, Enger PØ, Terzis JA, Bjerkvig R. A novel eGFP-expressing immunodeficient mouse model to study tumor-host interactions. *FASEB J* 2008;22: 3120–8.
27. Demuth T, Rennert JL, Hoelzinger DB, Reavie LB, Nakada M, Beaudry C, Nakada S, Anderson EM, Henrichs AN, McDonough WS, Holz D, Joy A, et al. Glioma cells on the run—the migratory transcriptome of 10 human glioma cell lines. *BMC Genomics* 2008;9:54.
28. Mariani L, Beaudry C, McDonough WS, Hoelzinger DB, Demuth T, Ross KR, Berens T, Coons SW, Watts G, Trent JM, Wei JS, Giese A, et al. Glioma cell motility is associated with reduced transcription of proapoptotic and proliferation genes: a cDNA microarray analysis. *J Neurooncol* 2001;53:161–76.
29. Bellail AC, Hunter SB, Brat DJ, Tan C, Van Meir EG. Microregional extracellular matrix heterogeneity in brain modulates glioma cell invasion. *Int J Biochem Cell Biol* 2004;36:1046–69.
30. Sahai E. Mechanisms of cancer cell invasion. *Curr Opin Genet Dev* 2005;15:87–96.
31. Sameni M, Elliot E, Ziegler G, Fortgens PH, Dennison C, Sloane BF. Cathepsins B and D are localised at the surface of human breast cancer cells. *Pathol Oncol Res* 1995;7:43–53.
32. Kim KJ, Wang L, Su YC, Gillespie GY, Salhotra A, Lal B, Laterra J. Systemic anti-hepatocyte growth factor monoclonal antibody therapy induces the regression of intracranial glioma xenografts. *Clin Cancer Res* 2006;12:1292–8.
33. Saidi A, Hagedorn M, Allain N, Verpelli C, Sala C, Bello L, Bikfalvi A, Javerzat S. Combined targeting of interleukin-6 and vascular endothelial growth factor potently inhibits glioma growth and invasiveness. *Int J Cancer* 2009;125: 1054–64.
34. Parker BS, Ciocca DR, Bidwell BN, Gago FE, Fanelli MA, George J, Slavin JL, Möller A, Steel R, Pouliot N, Eckhardt BL, Henderson MA, et al. Primary tumour expression of the cysteine cathepsin inhibitor Stefin A inhibits distant metastasis in breast cancer. *J Pathol* 2008;214: 337–46.
35. Strojnik T, Zajc I, Bervar A, Zidanik B, Golouh R, Kos J, Dolenc V, Lah T. Cathepsin B and its inhibitor stefin A in brain tumors. *Pflugers Arch* 2000;439(3 Suppl):R122–R123.
36. Lah TT, Kos J, Blejec A, Frković-Georgio S, Golouh R, Vrhovec I, Turk V. The expression of lysosomal proteinases and their inhibitors in breast cancer: possible relationship to prognosis of the disease. *Pathol Oncol Res* 1997;3:89–99.
37. Kuopio T, Kankaanranta A, Jalava P, Krongvist P, Kotkansalo T, Weber E, Collan Y. Cysteine proteinase inhibitor cystatin A in breast cancer. *Cancer Res* 1998;58:432–6.
38. Sinha AA, Quast BJ, Wilson MJ, Fernandes ET, Reddy PK, Ewig SL, Gleason DF. Prediction of lymph node metastasis by the raio of cathepsins B to Stefi A in patients with prostate carcinoma. *Cancer* 2002;94:3141–49.
39. Ehtesham M, Winston JA, Kabos P, Thompson RC. CXCR4 expression mediates glioma cell invasiveness. *Oncogene* 2006;25:2801–6.
40. Strojnik T, Kavalar R, Zajc I, Diamandis EP, Oikonomopoulou K, Lah TT. Prognostic impact of CD68 and kallikrein 6 in human glioma. *Anticancer Res* 2009;29:3269–79.
41. Colin C, Voutsinos-Porche B, Nanni I, Fina F, Metellus P, Intagliata D, Baeza N, Bouvier C, Delfino C, Loundou A, Chinot O, Lah T, et al. High expression of cathepsin B and plasminogen activator inhibitor type-1 are strong predictors of survival in glioblastomas. *Acta Neuropathol* 2009; 118:745–54.
42. Bervar A, Zajc I, Sever N, Katunuma N, Sloane BF, Lah TT. Invasiveness of transformed human breast epithelial cell lines is related to cathepsin B and inhibited by cysteine protease inhibitors. *Biol Chem* 2003;384:447–55.
43. Gocheva V, Zeng W, Ke D, Klimstra D, Reinheckel T, Peters C, Hanahan D, Joyce JA. Distinct roles for cysteine cathepsin genes in multistage tumorigenesis. *Genes Dev* 2006;20:543–56.
44. Dennhöfer R, Kurschat P, Zigrino P, Klose A, Bosserhoff A, van Muijen G, Krieg T, Mauch C, Hunzelmann N. Invasion of melanoma cells into dermal connective tissue *in vitro*: evidence for an important role of cysteine proteases. *Int J Cancer* 2003;106:316–23.